*35th EPS Conference on Plasma Phys. Hersonissos, 9 - 13 June 2008 ECA Vol.**32D**, P-1.072 (2008)*

Beta Limits and Edge Stability for Negative Triangularity Plasmas in the TCV Tokamak

S.Yu.Medvedev[1], A.A.Ivanov[1], A.A.Martynov[1], Yu.Yu.Poshekhonov[1],
R.Behn[2], Y.R.Martin[2], A.Pochelon[2], O.Sauter[2], L.Villard[2]

[1]*Keldysh Institute, Russian Academy of Sciences, Moscow, Russia*

[2] *Ecole Polytechnique Fédérale de Lausanne (EPFL), Centre de Recherches en Physique des Plasmas (CRPP), Association Euratom-Confédération Suisse, Lausanne, Switzerland*

In L-mode TCV tokamak discharges the electron heat transport has been found to decrease towards negative triangularity [1], leading to a factor of two improvement in confinement from $\delta = 0.4$ to -0.4. This trend of confinement with triangularity in L-mode stands in opposition to H-mode confinement, where the confinement improves with increasing positive triangularity (ASDEX-UPGRADE, JET), due to pedestal pressure increase with positive triangularity. Also, ELM induced heat loads are a severe threat for the first wall of a reactor. It is thus crucial to find ways to reduce or to avoid large ELMs. Varying the triangularity, inclusive over the negative triangularity range, will bring new elements to H-mode physics and transport.

The beta limits against both localized Mercier and ballooning modes and global pressure driven kink modes are lower for negative triangularity configurations. However, it gives a possibility to study resistive wall modes at lower power.

When the X-point is placed on the LFS, where the curvature of the magnetic field lines is unfavorable, the current density needed to access the second stability domain increases significantly and may even exclude it altogether. The edge kink-ballooning mode stability limits follow the changes in the high-n limits behavior [2]. It gives lower pressure pedestal height attainable in the negative triangularity configurations. It could potentially lead to different ELM behaviors in positive and negative triangularity configurations.

1 Free boundary equilibria and vertical stability

Although TCV is capable of generating plasma cross sections with a large variety of shapes, including negative triangularity and X-points, certain combinations are excluded by technical constraints. In particular, for diverted configurations, the strike points should be placed in regions covered by graphite tiles, which can support the local power densities. Placing strike points on the LFS wall is critical, since the presence of diagnostic ports restricts the zones with full toroidal coverage (highlighted in red in Figure 1). The combination of negative and positive triangularity (at the top and bottom, respectively), results in a plasma configuration with strike points on the central column, with the capability to handle high power densities. Furthermore, the X-point is located in the region of favorable curvature of the B-field lines. Changing the elongation, there is a possibility to shift such an equilibrium to adapt the upper quasi X-point to the upper corner ring with toroidally continuous coverage. Free-boundary equilibria for the plasma current $I_p = 380kA$ calculated with the SPIDER code are presented in Figure 1.

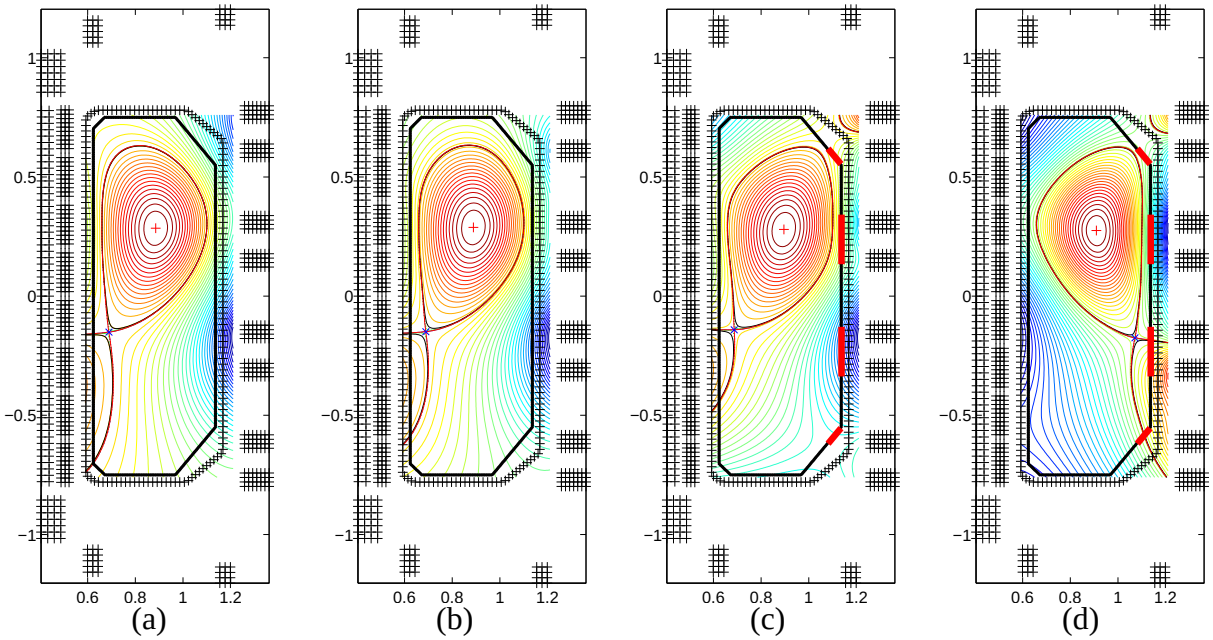

Figure 1. Poloidal flux level lines for free boundary equilibria in TCV tokamak. Plasma elongation $\kappa \sim 1.8$*. Triangularity upper/lower (a)* $\delta = 0.3/0.8$*, (b)* $\delta = 0.05/0.8$*, (c)* $\delta = -0.4/0.8$*, (d)* $\delta = -0.5/-0.8$*.*

The equilibrium calculations for the plasma cross sections shown in Figure 1 were based on pressure profiles typical for ohmic H-mode conditions in TCV [4]. However, experimental results are only available for case (a) (positive triangularity). Variations of the basic profiles (B,C,D in Figure 2) have been used to investigate the influence of pressure profiles on the stability limits. With the elongation $\kappa \sim 1.8$, plasma radius $a \sim 0.22m$, the plasma vertical stability is rather sensitive to the upper triangularity (Figure 3). The upper and lower negative triangularity case demonstrates the highest $n = 0$ mode growth rates $\gamma \sim 300 - 1500s^{-1}$. Moreover, the value of γ strongly depends on the proximity of the plasma to the LFS wall in this case.

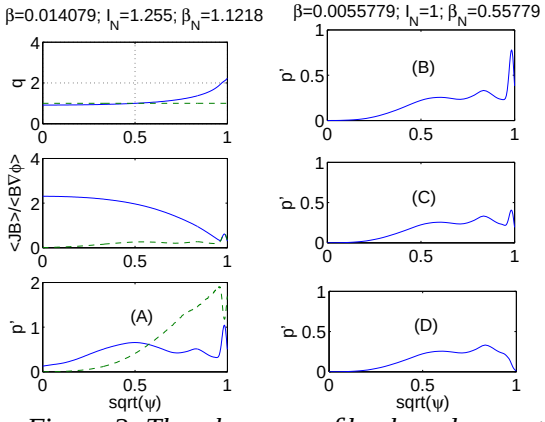

Figure 2. The plasma profiles based upon the reconstructed electron temperature and density profiles for the TCV shot #26383 (dashed lines show bootstrap current and ballooning mode limit for pressure gradient) (A) and the pressure gradient profiles with low core values used for beta limit calculations: pedestal (B), half-pedestal (C), no pedestal (D).

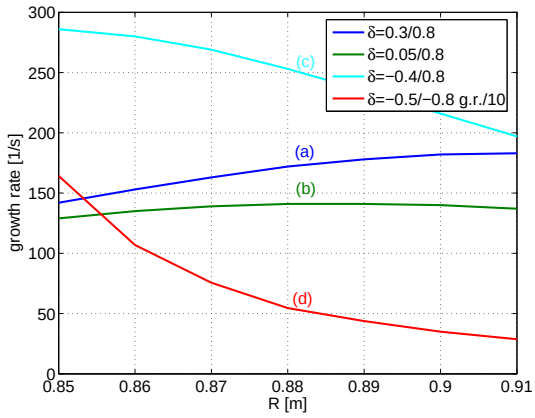

Figure 3. Vertical instability growth rates calculated with the KINX-NW code for the TCV equilibria with different triangularity versus the plasma center radius; $R = 0.88m$ *is the TCV center. The growth rates for* $\delta = -0.5/-0.8$ *configuration are divided by 10 for the plot. Labels (a),(b),(c),(d) refer to the equilibria shown in Figure 1.*

2 Beta limits

For the equilibria with upper negative triangularity, Mercier modes sets quite low stability threshold for the pressure gradient in the plasma core. In agreement with the large aspect ratio Mercier criterion including shape effects [5], increasing safety factor is not always stabilizing for negative triangularity case and the limiting pressure gradient mostly depends on the value of shear also for $q > 1$. Making the pressure gradient smaller in the core stabilizes the localized modes there (Figure 2, right).

The pressure driven kink mode limits were computed for the equilibrium series shown in Figure 1, keeping the parallel current profile fixed and re-scaling the pressure gradient. Table 1 gives the beta limits against the kink modes with the toroidal wave numbers $n = 1, 2, 3$ calculated with the KINX code for the four plasma shapes of Figure 1 and the four pressure profiles of Figure 2. The beta limits are much lower in the negative triangularity configurations and the limits for global modes decrease for large values of the pressure gradient in the pedestal, while the limits for plasmas with positive triangularity (cases a and b) are less sensitive to the pedestal profiles.

n	δ top/bot	no pedestal(B)	half pedestal(C)	pedestal(D)	pedestal+core(A)
1/2/3	0.3/0.8	2.73/3.25/ 3.69	2.95/3.41/3.54	2.96/3.14/2.99	3.98/4.04/3.95
1/2/3	0.05/0.8	2.27/2.88/3.25	2.34/2.93/3.10	2.34/2.64/2.48	2.64/3.08/3.07
1/2/3	-0.4/0.8	1.40/2.04/2.23	1.45/1.86/1.89	1.30/1.43/1.31	1.28/1.51/1.16
1/2/3	-0.5/-0.8	1.37/1.98/1.70	1.42/2.15/1.95	0.87/1.28/0.98	1.57/2.05/1.56

Table 1. Normalized β_N values for different plasma triangularity and pedestal pressure profiles. Normalized current value $I_N = 1.0$, $q_0 > 1.1$. The labels of the profiles refer to Figure 2.

3 Edge stability

The effect of a plasma boundary shape deformation involving a local poloidal curvature increase at the LFS was studied in [2]. Here, placing an X-point at the LFS has a similar but stronger effect on the access to the second stability domain because of the larger deformation.

The edge stability diagrams (Figure 4) were computed by the KINX code for series of equilibria with independently re-scaled parallel current density $J_{||}$ (normalized by the averaged value over the plasma cross-section $< J >$) and pressure gradient (normalized by the ballooning limit p'_c at the plasma edge) in the pedestal. In case of negative triangularity the access to the second stability region of ballooning modes is closed: for high values of the parallel current density close to the shear reversal multiple Mercier modes become unstable for upper and lower negative triangularity even at very low pressure gradients. All the stability limits shift to lower values of the pressure gradient for the negative triangularity cases. Moreover, fixed boundary modes with medium toroidal wave numbers $n \sim 10$ go unstable together with high-n ballooning modes and free boundary edge kink/ballooning modes for the case of upper and lower negative triangularity.

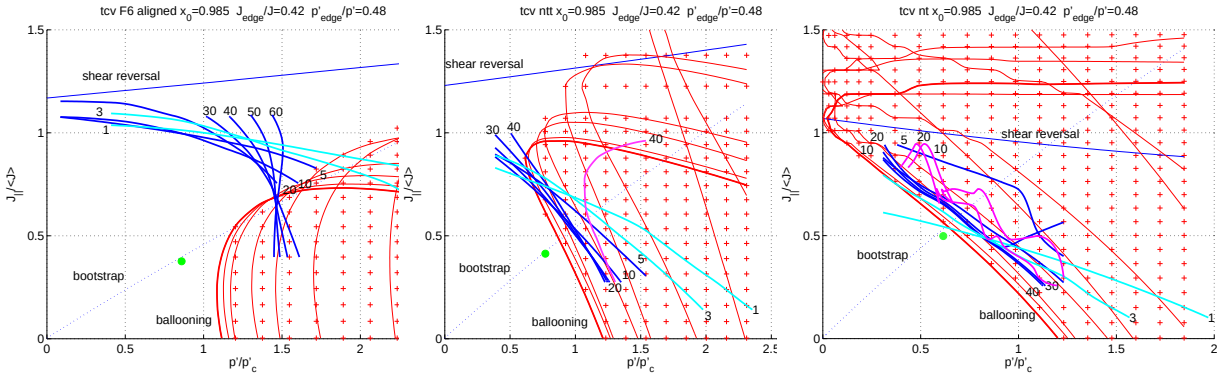

Figure 4. The edge stability diagrams for the TCV configuration with different triangularity: (b) $\delta = 0.05/0.8$, (c) $\delta = -0.4/0.8$, (d) $\delta = -0.5/-0.8$. The crosses and thin lines show the high-n ballooning mode stability boundaries (overall through the whole pedestal and for individual magnetic surfaces respectively). Bold lines give the stability boundaries for edge kink/ballooning modes (toroidal wave numbers are shown). The green circle shows the pedestal parameters for the basic equilibrium with the profiles from Figure 2 (left). The cyan lines show the global $n = 1, 3$ mode limits for the normalized current value $I_N = 1$ corresponding to $q_0 > 1.1$. Magenta lines show the limits against fixed boundary modes.

4 Conclusions

The plasma ideal MHD stability properties change significantly in the negative triangularity tokamak configurations:

- vertical instability growth rates increase with negative triangularity and become very sensitive to the proximity of plasma to the LFS wall in the case of upper and lower negative triangularity;
- localized Mercier modes are unstable in the plasma core even for q_0 well above 1 when the upper triangularity becomes negative;
- beta limits against global pressure driven kink modes are lower and deteriorate with increase of the pressure gradient in the pedestal;
- second stability access closes for the edge kink ballooning modes and lower values of pressure gradient in the pedestal are needed to drive them unstable.

The performed studies are certainly very valuable as a preparation for planned experiments on TCV to investigate H-mode plasmas at negative triangularity (type of ELMs, confinement properties, pedestal parameters etc). A configuration (with negative triangularity at the top) is suggested, which avoids an X-point on the LFS and strike points on the outside wall.

[1] Y. Camenen *et al.* Nuclear Fusion **47** (2007) 510

[2] S.Yu.Medvedev *et al.* Edge Stability and Boundary Shaping in Tokamaks. 34th EPS Conference on Plasma Phys. Warsaw, 2 - 6 July 2007 ECA Vol.31F, P-4.078 (2007)

[3] A.A.Ivanov *et al.* 32nd EPS Conf. on Plasma Phys., ECA Vol.29C, P-5.063 (2005)

[4] R.Behn *et al.* Plasma Phys. Control. Fusion **49** (2007) 1289

[5] H.Lütjens *et al.* Nuclear Fusion, **32** (1992) 1625

Acknowledgements The CRPP authors are supported in part by the Swiss National Science Foundation.